Study of Cationic Ring-Opening Photopolymerizations Using Optical Pyrometry

J. V. Crivello, B. Falk, M. R. Zonca, Jr.

Department of Chemistry, Rensselaer Polytechnic Institute, 110 8th Street, Troy, New York 12180-3590

ABSTRACT: Studies of the photoinitiated cationic ring-opening polymerizations of epoxide and oxetane monomers were conducted using optical pyrometry. Using this technique, the temperature of these photopolymerizations was monitored as a function of time. The effects of photoinitiator type and monomer structure on the rates of photopolymerization were investigated. Optical pyrometry was also used to investigate the acceleration of the photopolymerizations of various epoxide and oxetane monomers. Certain mixtures of monomers displayed synergistic effects that markedly increased their overall rates of polymerizations. In all cases in which acceleration of polymerization rate was noted, it could be attributed to an increase in the speed of ring opening of the initially formed protonated cyclic ether. The effects of relative humidity on the rate of cationic ring-opening photopolymerizations of cyclic ether monomers were also investigated. © 2004 Wiley Periodicals, Inc. J Appl Polym Sci 92: 3303–3319, 2004

Key words: photopolymerization; cationic polymerization; ring-opening polymerization; kinetics (polym.); optical pyrometry
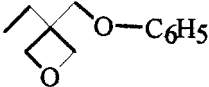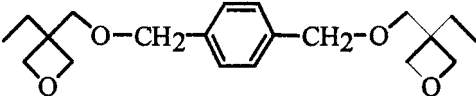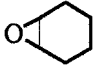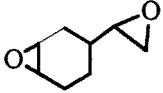
INTRODUCTION
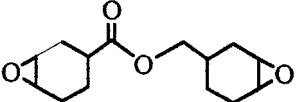
Photoinitiated cationic ring-opening polymerizations of heterocyclic monomers, such as epoxides and oxetanes, have found widespread use in UV curing applications. The chemical, mechanical, and processing requirements for these applications are very demanding. Further, for such uses as printing inks and protective coatings for metals, the photopolymerizations of these monomers must take place very rapidly to convert a liquid substrate to an insoluble polymer. Typically, the photopolymerizations used in these applications are carried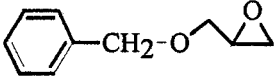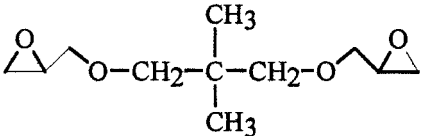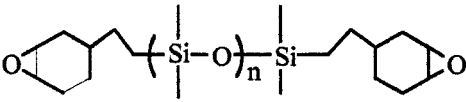 out using automated, in-line systems in which the photocurable substrate is typically subjected to UV light for an exposure time of a fraction of a second to 1 s. During that time, a liquid multifunctional monomer must undergo an efficient crosslinking polymerization reaction that consumes a great portion of the available polymerizable functional groups. To obtain the desired combination of mechanical and chemical properties, together with the mandatory high polymerization rates, it is common to use a complex mixture of monomers, photoinitiators, and additives. The photopolymerization behavior of such complex mixtures is difficult to monitor using existing analytical techniques.

Real-time infrared spectroscopy (RTIR)[1–3] and differential scanning photocalorimetry (DSP)[4,5] are the most often used analytical techniques for following the progress of photopolymerization reactions used in UV curing applications. These two techniques work well when they are used for the polymerization of simple one or two monomer component systems. They are less easily applied to systems in which more complex multicomponent mixtures of monomers of different reactivity are involved. Further, the latter two analytical techniques are comparatively slow and labor intensive and use expensive instrumentation. As a consequence, they are rarely used in an industrial setting for the optimization of photocurable formulations.

In a recent publication[6] we described preliminary results in monitoring both free-radical and cationic photopolymerizations using a new analytical technique, optical pyrometry. Using optical pyrometry (OP), the temperature of a liquid film of a monomer or mixture of monomers undergoing photopolymerization is monitored as a function of time. We have shown that the increase of temperature of such a sample can be directly related to a corresponding increase in the conversion of the monomer undergoing polymerization. OP is a highly sensitive, reproducible, and rapid analytical method. In this article, we report the results of a study of the effects of various experimental and compositional parameters of the photoinitiated cationic ring-opening polymerizations of epoxide and oxetane monomers using the OP technique.

TABLE I
Structures of Monomers

POX
3-ethyl-3-[(phenoxy)methyl]oxetane

XDO
1,4-bis[(3-ethyl-3-oxetanylmethoxy)methyl]-benzene

CHO
cyclohexene oxide

VCHDO
4-vinyl-1-cyclohexene dioxide

ERL-4221E
3,4-epoxycyclohexylmethyl 3′, 4′-epoxycyclohexane carboxylate

BGE
benzyl glycidyl ether

NDGE
neopentyl glycol diglycidyl ether

$n = 1, 3, 5$
$n = 1 = PC\text{-}1000$

DVE-3
triethylene glycol divinyl ether

EXPERIMENTAL

Materials

All organic starting materials and reagents used in this investigation were reagent quality and were used as purchased unless otherwise noted. The oxetane monomers 3-ethyl-3-[(phenoxy)methyl]oxetane (POX) and 1,4-bis[(3-ethyl-3-oxetanylmethoxy)methyl]-benzene (XDO) used in this work were kindly provided as gifts from the Toagosei Chemical Co. (Nagoya, Japan). Neopentylglycol diglycidyl ether, benzyl glycidyl ether, 4-vinyl-1,2-cyclohexene dioxide, and cyclohexene oxide were used as obtained from the Aldrich Chemical Co. (Milwaukee, WI). A sample of triethylene glycol divinyl ether (DVE-3) was provided by the GAF Chemicals Corp. (Wayne, NJ). 3,4-Epoxycyclohexylmethyl 3′,4′epoxycyclohexane carboxylate (ERL-4221E) was a product of the Union Carbide Corp. (Bound Brook, NJ). 1,6-Hexandiol divinyl ether was obtained as a sample from the BASF Corp. (Ludwigshaven, Germany). The synthesis of PC-1000 and that of the other silicone epoxides were prepared as previously reported.[6] The diaryliodonium salt photoinitiators used in this work were prepared as described in an earlier publication[7] from this laboratory.

Given in Table I are the names, abbreviations, and structures of the monomers used during the course of this study.

Optical pyrometry

The basic optical pyrometry apparatus and method used for monitoring the photopolymerizations carried out in this investigation were described in a recent communication.[6] The apparatus has undergone considerable modification and the configuration of the current instrument is shown in Figure 1. An Omega OS552-V1-6 industrial infrared thermometer (Omega Engineering, Inc., Stamford, CT), equipped with a laser-sighting device (OS550-LS), was mounted at the top of a 40 × 35 × 35 cm smoky gray acrylic irradiation cabinet. This instrument has a sensitivity of ±1°C with an operating temperature range of −18 to 538°C. Using the laser aligner, the focal point of the sensor of the OP instrument was centered in the middle of the sample window. At this location (15.2 cm from the infrared sensor), the focal spot diameter was 3.9 mm. Also mounted at the top of the cabinet was an acrylic cylinder that was bored to accommodate the probe end of a liquid optic cable. UV light was supplied to the sample chamber by a UVEX Model SCU-110 mercury lamp, equipped with a 95 cm liquid light pipe and directed onto the sample stage at a 45° angle (Costa Mesa, CA). Because of the selective absorption of the light pipe, the radiation transmitted at the sample stage consisted chiefly of wavelengths greater than 300 nm. The light intensity was modified by varying the distance of the fiber optic probe from the sample. The intensity of UV irradiation was measured with a control cure radiometer (UV Process Supply Inc., Chicago, IL). Various light intensities and irradiation times were used in the studies reported here and are noted in the individual figure captions.

The sample stage consisted of a platform that was milled to accept a 2 × 2 cm plastic slide frame. This provided a means of reproducibly fixing the position of the sample in the irradiation cabinet. The atmosphere and humidity under which the photopolymer-
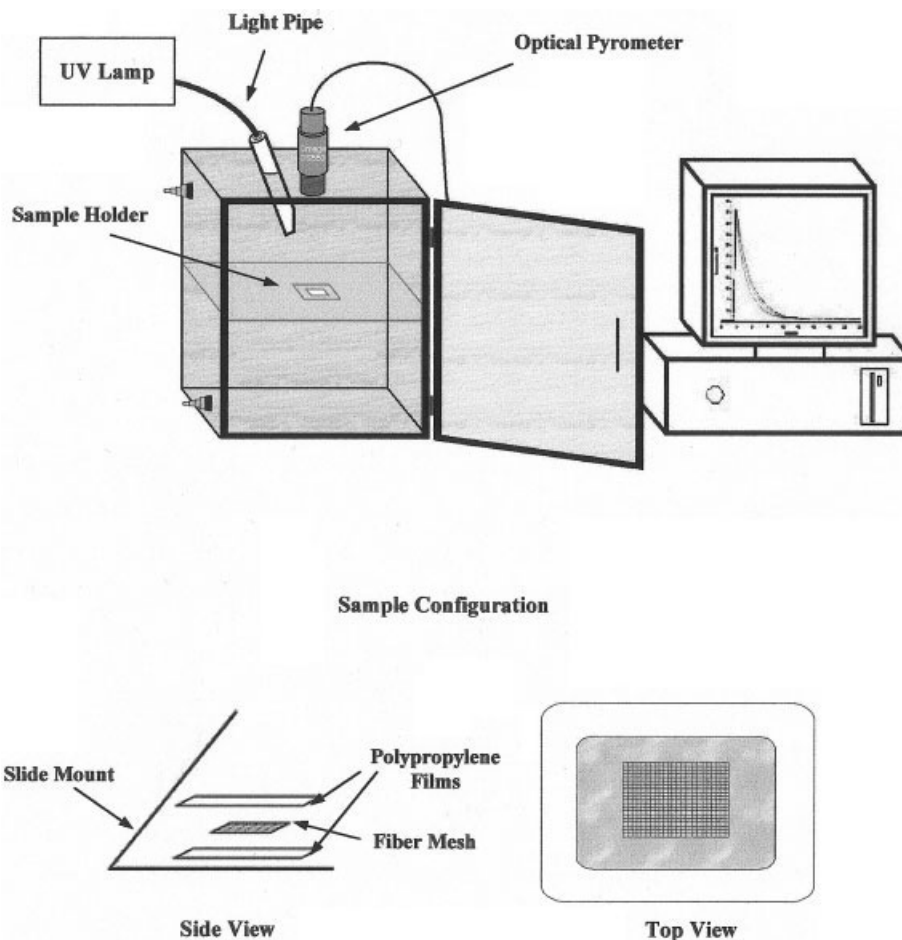
Figure 1 Optical pyrometry (OP) apparatus and sample configuration for the study of photopolymerizations.

izations were carried out could be controlled using the gas inlets fitted into the instrument cabinet. The apparatus also incorporated a heater for studies of the effects of temperature on cationic and free-radical photopolymerizations.
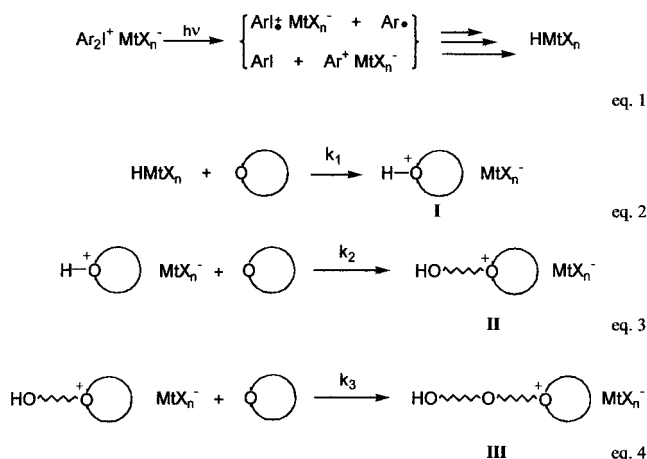
Samples for kinetic analysis were prepared as follows: homogeneous solutions of the desired monomer with a designated photoinitiator were prepared (all concentrations are given in mol % with respect to functional groups unless otherwise noted). A 10 μm corona-treated oriented poly(propylene) (PP) film (General Electric Corp., Hudson Falls, NY) was first laid down and a thin polyester fiber mesh was placed on top of the plastic film to serve as a spacer. The liquid sample was pipetted onto this assembly and an identical layer of PP film was placed over the top. In this manner, a reproducible liquid monomer layer 0.912 mm in thickness was obtained and, at the same time, because of its low volume and thermal mass, the fiber mesh did not affect the temperature of the polymerization reaction. The resulting sample sandwich was mounted in the plastic slide holder for UV irradiation. All optical pyrometer experiments made in this investigation were conducted at ambient temper-

ature (25–28°C), except where indicated, and at such light intensities as to permit a convenient analysis of the data. Before the start of the UV irradiation, the samples were allowed to equilibrate and establish a flat temperature baseline for 20 s. Temperature data were collected at a rate of 1 measurement/s and directly recorded and downloaded to an IBM 350-P137 personal computer for analysis.

Humidity experiments were carried out at ambient temperature by passing air through the closed irradiation chamber that was first saturated with water by bubbling through a water trap. This was continued until the desired relative humidity was attained, as measured using a humidity/temperature monitor (Fisher Scientific, Pittsburgh, PA). Samples were run without top film covers to permit equilibration with the humid environment.

Simultaneous OP and RTIR

As described previously[6] a Midac M-1300 FTIR spectrometer, equipped with a liquid nitrogen-cooled mercury–cadmium–telluride detector, was fitted with a

$$Ar_2I^+ MtX_n^- \xrightarrow{h\nu} \left\{ \begin{array}{l} ArI^+ \cdot MtX_n^- + Ar\cdot \\ ArI + Ar^+ MtX_n^- \end{array} \right\} \Longrightarrow HMtX_n \qquad \text{eq. 1}$$

$$HMtX_n + \langle O \rangle \xrightarrow{k_1} H\!-\!\overset{+}{O}\langle \rangle \; MtX_n^- \qquad \text{eq. 2}$$
$$\mathbf{I}$$

$$H\!-\!\overset{+}{O}\langle \rangle \; MtX_n^- + \langle O \rangle \xrightarrow{k_2} HO\!\sim\!\!\sim\!\overset{+}{O}\langle \rangle \; MtX_n^- \qquad \text{eq. 3}$$
$$\mathbf{II}$$

$$HO\!\sim\!\!\sim\!\overset{+}{O}\langle \rangle \; MtX_n^- + \langle O \rangle \xrightarrow{k_3} HO\!\sim\!\!\sim\!\!\sim\!O\!\sim\!\!\sim\!\overset{+}{O}\langle \rangle \; MtX_n^- \qquad \text{eq. 4}$$
$$\mathbf{III}$$

Scheme 1

UVEX Model SCU-110 mercury lamp (Sunnyvale, CA) in which the light was carried through a flexible wand to the sample compartment. The end of the wand was placed at a predetermined distance and directed at an incident angle of 45° onto the sample window. For these experiments, the sample window and holder were also tilted at a 45° angle to the infrared beam. The optical pyrometer was mounted such that it was perpendicular to the sample and located as described above at such a distance so as to place the focal point at the sample plane. Sample preparation was the same as described for the OP studies, with the omission of the mesh spacer.

Both FT–RTIR and OP analytical methods were triggered at the same time by opening the shutter of the UV irradiation source. The FT–RTIR data were collected at a rate of one spectrum/s and the OP temperature data at the same rate. During the photopolymerization, a characteristic infrared absorption band of the functional group undergoing polymerization was monitored. Then, the conversion and thermal data were plotted together versus time using Midac Grams/386 and Excell software.

RESULTS AND DISCUSSION

Given in Scheme 1 is a general mechanism for the photoinitiated ring-opening polymerization of cyclic ether monomers such as epoxides and oxetanes. A diaryliodonium salt is shown in this mechanism as an example of a typical onium salt photoinitiator. It may be noted that there are a great number of variables that affect the overall rate and extent of such cationic ring-opening polymerizations. Among these may be mentioned, the nature of the photoinitiator, the character of the monomer or monomers used, the intensity and wavelength of the irradiating light, and the environmental conditions under which the photopolymerization is conducted. Several of these variables are interdependent. For example, to be effective, the photoinitiator must possess absorption characteristics that are complementary to the emission properties of the light source. As stated in the introduction, it was the object of this investigation to use optical pyrometry to examine the effects of some of these variables on the cationic photopolymerizations of epoxides and oxetanes.

Effect of the structure of the photoinitiator

The function of the photoinitiator in a cationic photopolymerization is to absorb light and then to undergo a photoinduced transformation that liberates a species capable of initiating the polymerization reaction. Onium salts have been well established as the most efficient photoinitiators of cationic polymerization. As shown above in Scheme 1, when photoinitiators such as diaryliodonium salts are subjected to UV irradiation [eq. (1)], they generate a protonic acid. Onium salts undergo photolysis by several different mechanisms. However, in all cases, the polymerization of the cyclic ether monomer takes place by first undergoing protonation [eq. (2)] and then ring opening by nucleophilic attack of monomer molecules on the protonated species [eq. (3)]. Finally, the chains grow by the repetitive addition of monomer molecules to the active chain end [eq. (4)]. There are a number of factors that determine the efficiency of a photoinitiator. Among these include (1) the quantum yield for acid generation, (2) the UV absorption characteristics of the photoinitiator, and (3) the character of the anion (i.e., the strength of the protonic acid that is generated). Shown in Figure 2 is a study of the photopolymerization of 3,4-epoxycyclohexylmethyl 3′,4′-epoxycyclohexanecarboxylate (ERL-4221E) that was carried out using five different types of onium salt photoinitiators bearing the SbF_6^- anion. The quantum yields and UV absorption characteristics of these onium salts are given in Table II. It is also important to point out that the UV irradiation that is delivered to these and all samples studied in this work contains only emission wavelengths above 300 nm. The fluid optic cable acts like a filter removing shorter UV wavelengths as well as infrared radiation.

Triarylsulfonium (P_4S) and thianthrenium salts (TX-OEt), with the highest absorption at long wavelengths, show the highest efficiency in the polymerization of this monomer. The dialkyl-4-hydroxyphenylsulfonium salt (C_4-4HPS) also displays excellent photoresponse. Less effective are the diaryliodonium salt (IOC10) and dialkylphenacylsulfonium salt (C_4C_{18}-DPS). The observed response of the photoinitiators depicted in Figure 2 can be rationalized based on the absorption characteristics of the photoinitiator at wavelengths above 300 nm and their quantum yields. Those photoinitiators with the greatest absorption
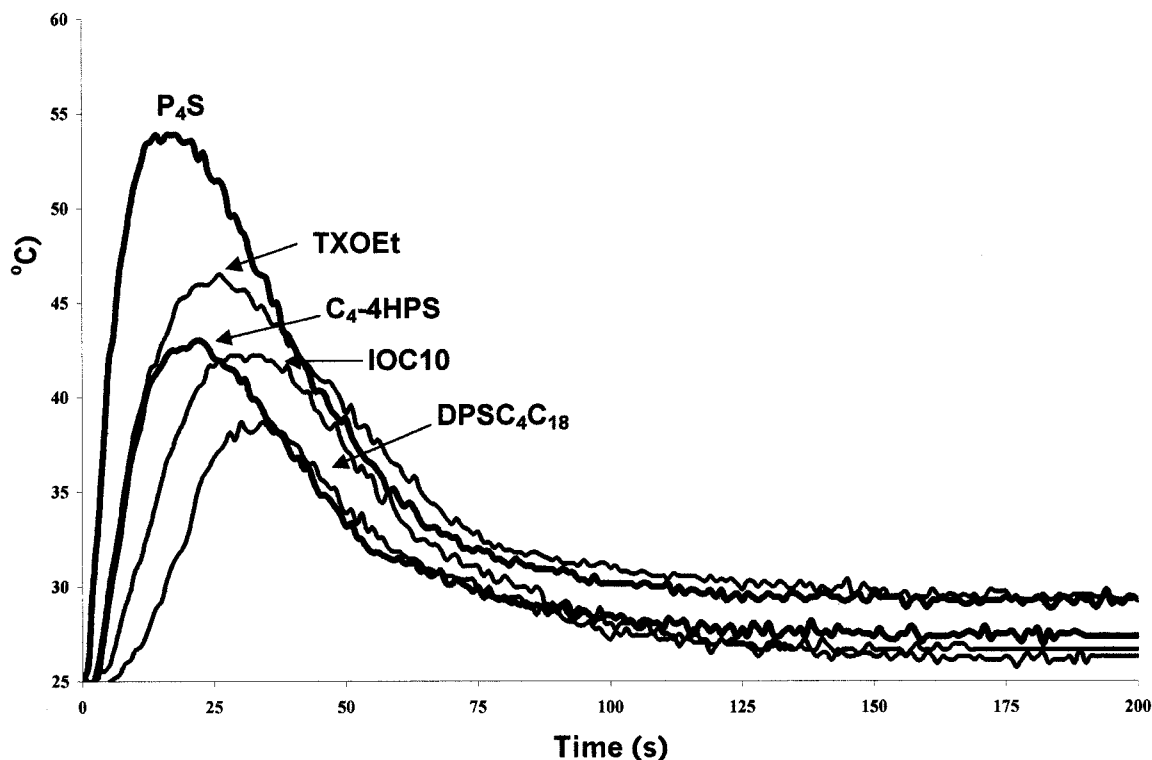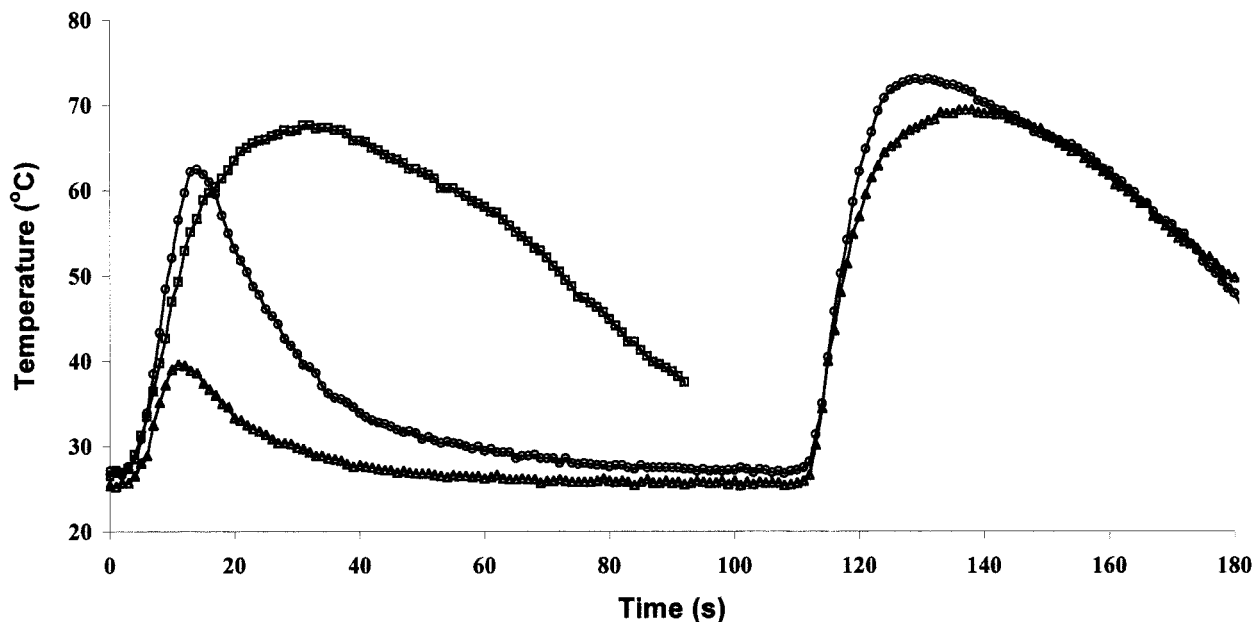
Figure 2 OP study of the photopolymerization of ERL-4221E using different onium salt photoinitiators (1.0 mol % photoinitiator, 1142 mJ cm^{-2} min^{-1}).

TABLE II
Quantum Yields and UV Absorption Characteristics for Onium Salt Photoinitiators

Notation	Structure	Quantum yield	UV bands (nm)	Ref.
IOC10 IOC15		0.4	247 (15,000)	1, 8
P$_4$S		—	225 (234,000) 300 (19,500)	9
TXOEt		—	202 (54,910) 250 (18,390) ≈310 (5840)	10
DPSC$_4$C$_{18}$		0.43	251 (12,000) 281 (1630)	11, 12, 13
C$_4$-4HPS		0.26	250 (11,700) 271 (3690) 281 (2170)	8, 14, 15

Figure 3 Study of the dark polymerization of cyclohexene oxide under various reaction conditions: continuous irradiation (□); irradiation discontinued at 60°C and restarted at 110 s (△); irradiation discontinued at 38°C and restarted at 110 s (○) (1.0 mol % C_4-4HPS photoinitiator, 300 mJ cm^{-2} min^{-1}).

generally displayed the highest efficiency in this study.

In theory, the generation of a strong acid in the presence of an epoxide or oxetane monomer should lead to a nonterminating ring-opening polymerization. This means that even when the UV irradiation ceases, polymerization continues in what is generally termed a "dark polymerization" or "dark cure." The presence of a dark polymerization is often observed in practice and results in a slow change in the chemical and mechanical properties of the final polymer film. The presence of a dark polymerization or dark cure can be either beneficial or detrimental depending on the specific situation. There has been little attempt to characterize the progress of dark cure in photoinduced cationic polymerizations. Several studies of the polymerizations of two epoxide monomers in the presence of different cationic photoinitiators were carried out using optical pyrometry to monitor the course of the dark polymerizations. The results are depicted in Figures 3 and 4.

Figure 3 shows the polymerization of cyclohexene oxide conducted under several irradiation conditions using C_4-4HPS as the photoinitiator. This photoinitiator undergoes photolysis by a reversible mechanism and it was expected that this system would display little dark polymerization. In the first curve, one can observe the results of the photopolymerization carried out under continuous UV irradiation. A broad curve was observed, indicating that photopolymerization takes place over an irradiation period of at least 100 s. The second curve shows what happens when irradia-

tion is discontinued at 12 s when the temperature of the sample reached 60°C. The polymerization continues only for a very short time with the temperature rising to 63°C and then the temperature of the sample falls as cooling sets in. Thereafter, the temperature of the sample again slowly approaches room temperature. When the UV irradiation is again switched on after 110 s, there is an immediate increase in the sample temperature to 73°C as polymerization of the monomer resumes. A similar curve is shown in Figure 3 in which the light is extinguished when the temperature of the sample reached 38°C (10 s) and then switched back on at 110 s. A similar response of the polymerizing system at this lower initial temperature is seen. These results indicate that, as expected, there is little observable dark polymerization taking place in this monomer–photoinitiator system.

Figure 4 shows a similar study in which the photopolymerization of monomer, 4-vinyl-1-cyclohexene dioxide (VCHDO), was carried out in the presence of the diaryliodonium salt IOC10. IOC10 undergoes irreversible fragmentation on photolysis and it was predicted that photopolymerizations conducted in the presence of this photoinitiator would display a considerable dark polymerization effect. Continuous irradiation produces a rapid and highly exothermic polymerization, with essentially complete conversion of the monomer, as indicated by the sharpness of the curve. Cooling is rapid even under continuous irradiation conditions. When the irradiation was terminated when the temperature reached 38 and 60°C (13 and 20 s), respectively, the polymerization continued for
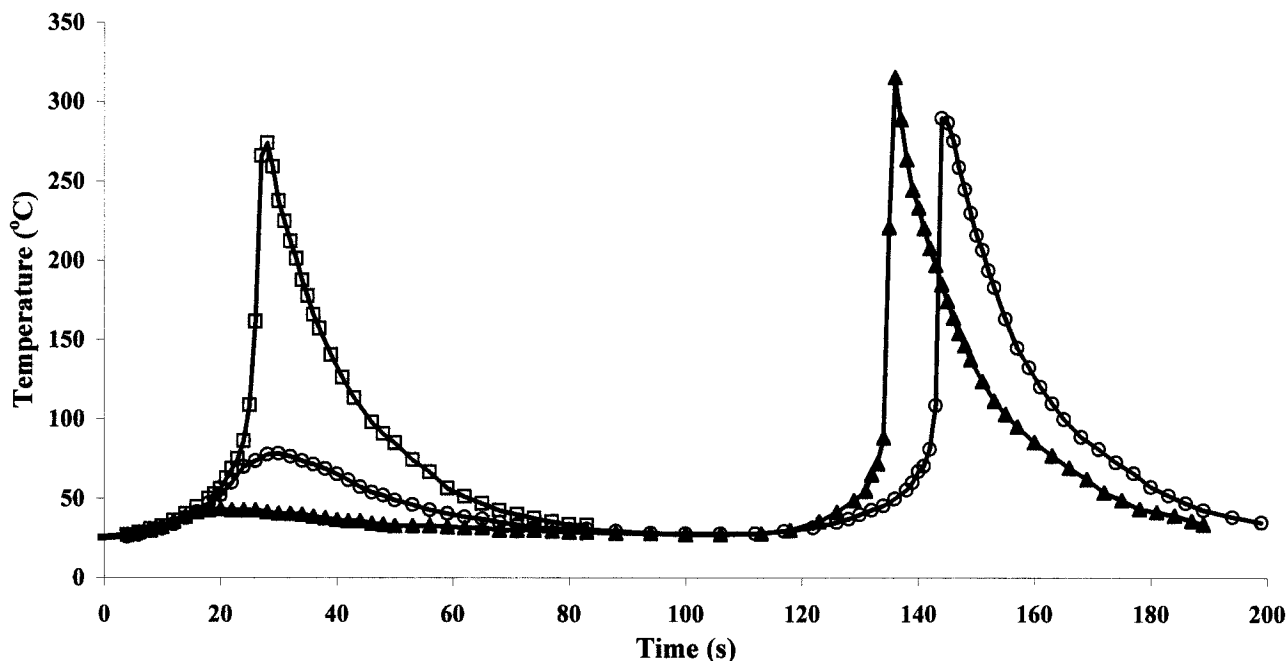
Figure 4   Study of the dark polymerization of 4-vinyl-1,2-cyclohexene dioxide under various reaction conditions: continuous irradiation ($\square$); irradiation discontinued at 60°C and restarted at 110 s ($\triangle$); irradiation discontinued at 38°C and restarted at 110 s ($\bigcirc$) (1.0 mol % IOC10 photoinitiator, 300 mJ cm^{-2} min^{-1}).

some time and slowly ceased, indicating appreciable dark polymerization. However, when UV irradiation was resumed after standing in the dark, polymerization again took place rapidly and exothermically. It appears that despite the difference in the mechanism of the photolysis of these two different types of photoinitiators, that in both cases, the ring-opening polymerizations of the epoxide monomers display some dark polymerization. However, if the irradiation is terminated at an early stage of the photopolymerization before appreciable monomer is consumed, the dark polymerization that takes place is inefficient and the overall conversion remains low.

The difference in maximum temperatures (63 and 270°C) recorded in Figures 3 and 4 for the photopolymerization of CHO and VCHDO are attributed not only to the fact that two very different photoinitiators with different quantum yields and mechanisms of photolysis and initiation were used but to additional factors that are related to the structure and properties of the monomers. The difunctional monomer VCHDO has a lower epoxy equivalent weight than that of CHO (70 versus 98 g/mol) that results in a higher polymerization temperature. In addition, during polymerization the thin film sample of CHO (bp 129–130°C) can be cooled through volatilization, whereas VCHDO (bp 110–113°C/20 mm) has a much higher boiling point and, because of crosslinking, is not easily volatilized.

Seeking to further validate the OP method, we conducted simultaneous RTIR measurements and OP on the same sample. This was accomplished by installing the OP device into the sample compartment of the FTIR spectrometer.[6] Double plots of the conversion versus time and temperature versus time for the polymerization of VCHDO are shown in Figure 5. To slow the polymerization somewhat, the photoinitiator (4-n-decyloxyphenyl)phenyliodonium hexafluorophosphate (IOC10 PF$_6$) was used for this study. There is a very good correlation between the initial slopes of the two curves and they nearly overlap with one another, signifying that there is a direct relationship between the conversion and the sample temperature. It may also be noted that the maximum temperature of the sample is attained as the conversion slows and reaches its maximum.

Study of the effects of monomer structure using OP

As noted earlier, the structure of a monomer has a pronounced effect on its reactivity in a cationic photopolymerization. It is well known that cycloaliphatic epoxides undergo ring-opening polymerization much more rapidly than other types of epoxide monomers.[16–18] In previous communications[19–21] from this laboratory, we reported that silicone epoxide monomers bearing epoxycyclohexyl groups display exceptional reactivity in photoinitiated cationic polymerization. Figure 6 shows the results of a study of the reactivity of a series of three related difunctional epoxy monomers, in which only the length of the dimethylsiloxane spacer was changed. As the chain
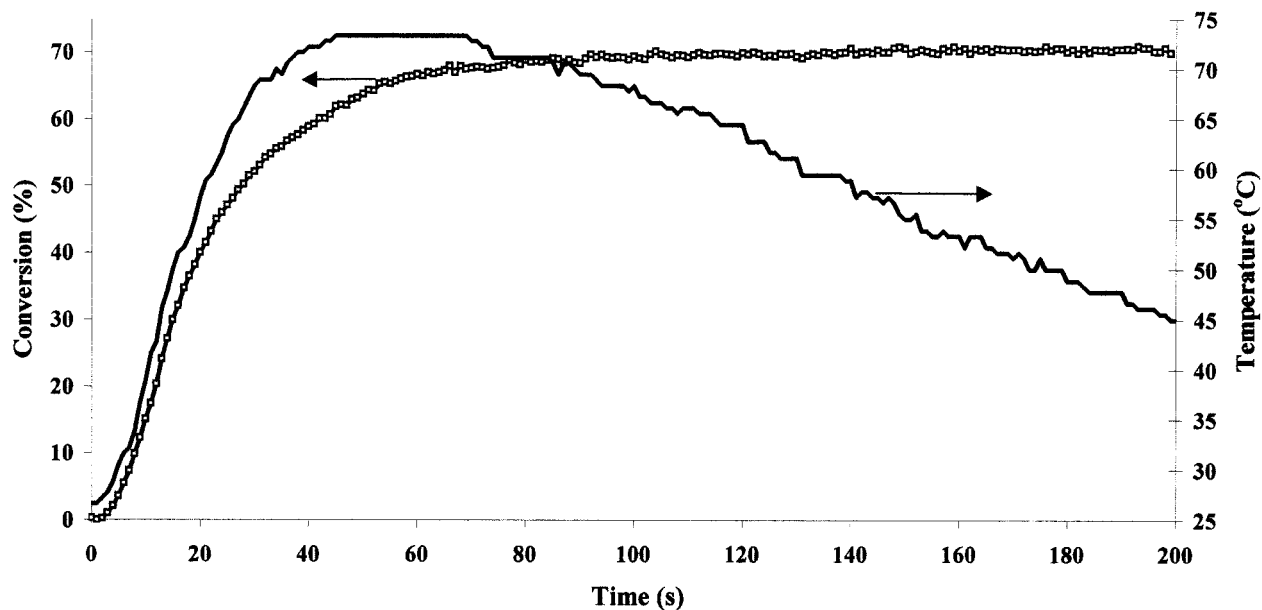
Figure 5 Simultaneous RTIR and OP studies of the photopolymerization of VCHDO using 1.0 mol % (4-*n*-decyloxyphenyl)phenyliodonium hexafluorophosphate at 999 mJ cm^{-2} min^{-1}.

length of the spacer increases, there is a corresponding decrease in the peak temperature attained by the monomer during photopolymerization. This correlates well with the decrease in the density of the reactive epoxycyclohexyl groups in these monomers with increasing chain length.

For many applications involving photopolymerizations, it is essential to achieve the most rapid conver-

sion possible of a liquid monomer to a crosslinked, solid polymer. The cationic ring-opening polymerizations of cyclic ethers are reasonably rapid processes for highly strained monomers such as epoxides and oxetanes. In most cases, however, they are slower than the corresponding photoinduced free-radical polymerizations of acrylate monomers. For these reasons, there is an ongoing need to develop strategies to find
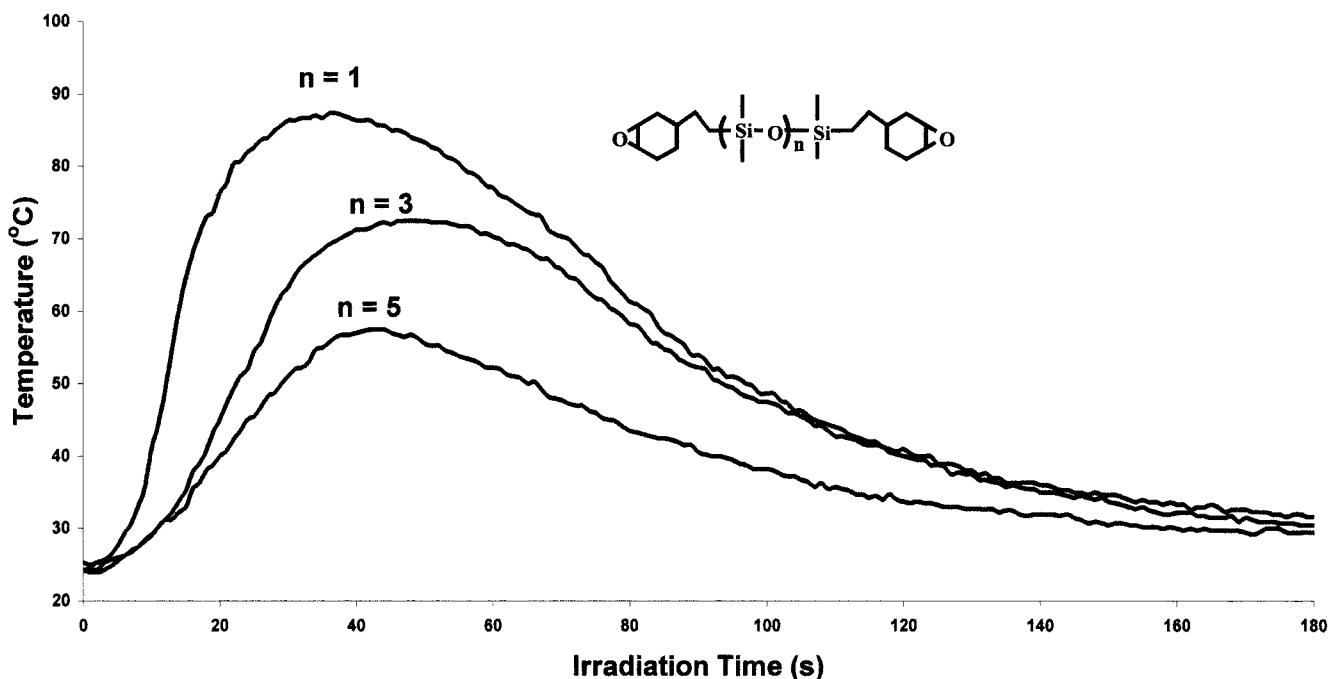
Figure 6 Effect of siloxane spacer length in three related silicone epoxy monomers (1.0 mol % IOC10 photoinitiator, 497 mJ cm^{-2} min^{-1}.
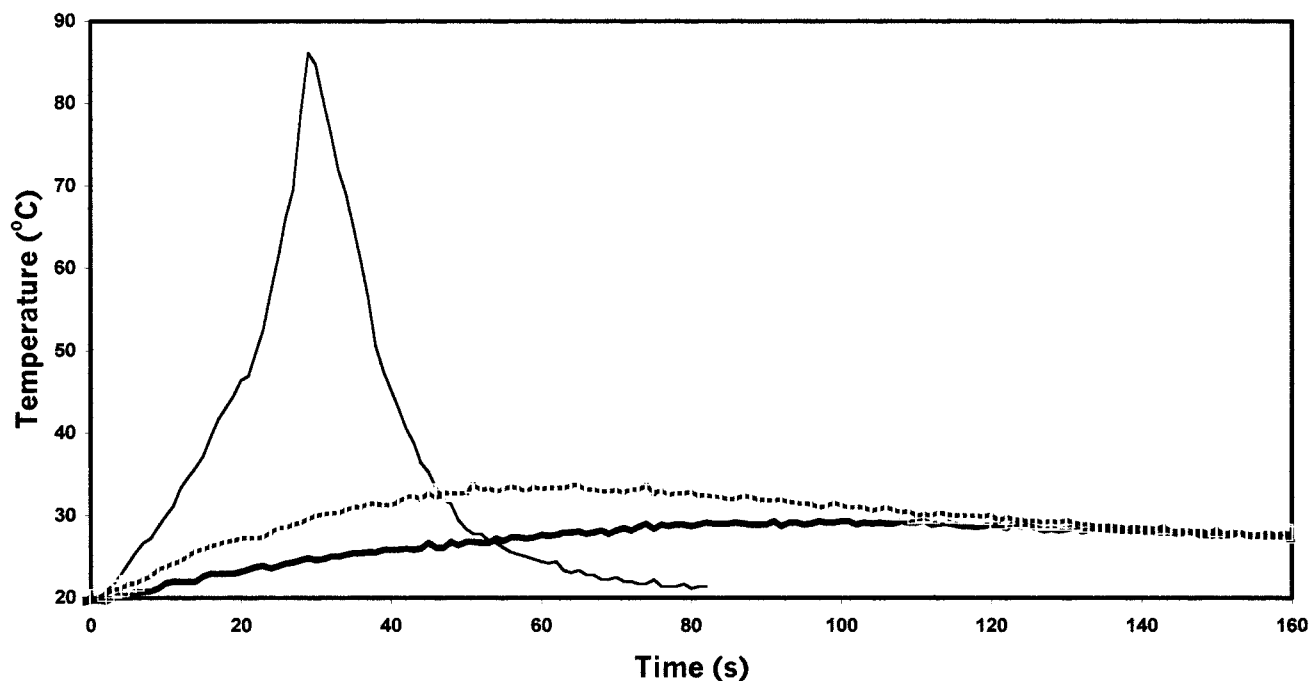
Figure 7 OP study of the effect of the addition of cyclohexene oxide (CHO) to the photopolymerization of benzyl glycidyl ether: 0% (━); 2.0% (- - -); 10% (—) (1.0 mol % IOC15 photoinitiator, 496 mJ cm^{-2} min^{-1}).

means of accelerating the photoinitiated cationic polymerizations of heterocyclic ether monomers. Of course, the concentration of the photoinitiator and the light intensity play important roles in determining the overall rate of a photopolymerization. However, it has been found[22] that for any monomer system, both the photoinitiator concentration and the light intensity reach maximum values beyond which no further increase in rate can be achieved. At this point, other means of accelerating the rates of polymerization must be sought. Considering the general mechanism depicted in Scheme 1, it is important to elucidate which step in the sequence is the rate-determining step for the given monomer system under study. It is worthwhile to point out that only the first step [eq. (1)], the photogeneration of the strong Brønsted acid HMtX$_n$, is light dependent. All subsequent steps are nonphotochemical processes that proceed from the attack and propagation of catalytic amounts of highly reactive species (protons and oxonium ions) with the monomer. The photogenerated strong acid very rapidly protonates the cyclic ether (i.e., k_1 is large), as depicted in eq. (2). The secondary oxonium species (**I**) that is formed undergoes attack by the nucleophilic cyclic ether to yield the tertiary oxonium species (**II**) as a result of ring opening of the heterocyclic ring [eq. (3)]. Finally, attack by a cyclic ether monomer on the tertiary oxonium ion [eq. (4)] leads to chain growth (**III**). The rate constants k_2 and k_3, respectively, for eqs. (3) and (4) are different because the species involved, **I** and **II**, have different ring strains, steric interactions,

and electronic charge distributions. The relative magnitudes of k_2 and k_3 depend on the structure of the specific monomer undergoing polymerization. For example, in the cationic photopolymerization of highly strained cycloaliphatic epoxides both k_2 and k_3 are large and observation of the effects of the difference in rates is difficult. However, for other cyclic ether monomer systems either step 3 or step 4 may be rate limiting. Examples of both cases will be given in the course of these studies.

It has been noted that certain combinations of cyclic ether monomers exhibit a synergistic effect on the rates of polymerization of each other.[23] The use of such combinations can be adapted to good advantage in many potential applications. By use of the OP method, it is possible to rapidly screen and then optimize multicomponent monomer mixtures. Typically, such mixtures of monomers function by overcoming limitations to the overall rate of a polymerization that occurs when step 3 (i.e., $k_2 < k_3$) is rate limiting. Such a case is shown in Figure 7 for the cationic photopolymerization of benzyl glycidyl ether. When pure benzyl glycidyl ether is photopolymerized alone, the polymerization is extremely sluggish. The polymerization is characterized by only a very slight temperature rise, indicative of a very slow increase in conversion of monomer to polymer over an irradiation period of 160 s. Figure 7 shows the effect of adding different amounts of the highly reactive monomer, cyclohexene oxide (CHO), to benzyl glycidyl ether. The inclusion of 2 mol % of CHO results in a measur-
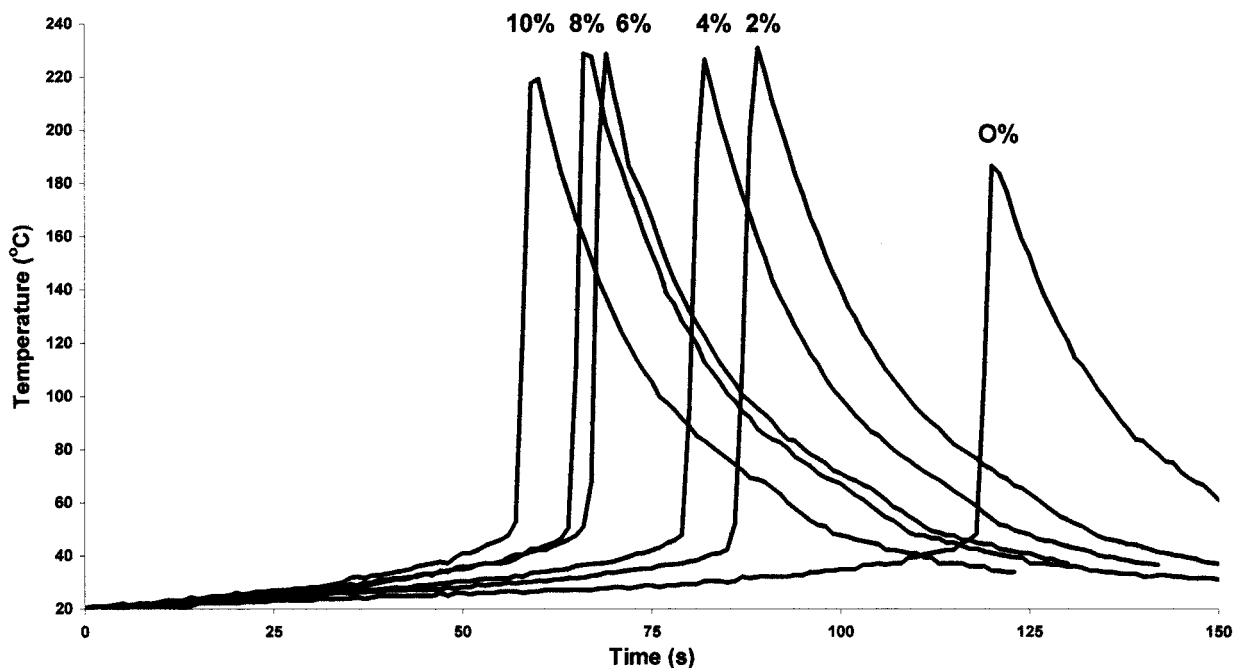
Figure 8 OP study of the photopolymerization of NPGE in the presence of various concentrations of VCHDO (1.0 mol % IOC15 photoinitiator, 860 mJ cm^{-2} min^{-1}).

able increase in the temperature of the photopolymerization of the benzyl glycidyl ether, indicating a higher polymerization rate compared to that of the pure monomer. Incorporation of 10 mol % of CHO produces a dramatic acceleration of the rate of polymerization of this monomer. Because CHO undergoes much faster ring opening than benzyl glycidyl ether, the protonated CHO **I** is rapidly converted to a tertiary oxonium species **II**. Thus k_2 is substantially increased, whereas the propagation rate constant k_3 for benzyl glycidyl ether is essentially unaffected.

Aliphatic glycidyl ethers display sluggish response to photoinitiated cationic polymerization even in the presence of the most reactive photoinitiators. At the same time, these monomers are attractive substrates for UV curing applications because they are easily prepared and inexpensive. Figure 8 depicts the photopolymerization of neopentylglycol diglycidyl ether (NPGE), carried out in the presence of 1.0 mol % IOC15. This polymerization proceeds only after a long induction period. However, when it does take place, the polymerization is extremely rapid and exothermic. These are characteristics that we attribute to a slow initial ring-opening step (i.e., $k_2 < k_3$). When the very highly reactive diepoxide monomer 4-vinyl-1-cyclohexene dioxide (VCHDO) is added to NPGE, the induction period is reduced in proportion to the amount of epoxide added. At the same time, the rapid, highly exothermic nature of the photopolymerization is preserved.

The commercially available monomer 3,4-epoxycyclohexylmethyl 3',4'-epoxycyclohexanecarboxylate (ERL-4221E) is the monomer of choice for many UV curable cationic formulations and is particularly useful for metal coatings. However, as shown in Figure 9, although the polymerization of this monomer takes place with only a very short induction period, it proceeds quite slowly. We discussed the reasons for the sluggish polymerization of this monomer in previous publications.[24,25] In Figure 9 are shown the results of an attempt to further enhance the rate of polymerization of this monomer through the addition of the even more reactive monomer limonene dioxide (LDO). There is only a slight increase in the rate of temperature increase on addition of up to 8 mol % of LDO to this monomer. This suggests that the slowest step in the polymerization of ERL-4221 is the propagation step [eq. (4) in Scheme 1; i.e., $k_2 > k_3$]. Because this is the case, addition of a minor amount of a second, more reactive monomer does not increase the overall polymerization rate of the major monomer component.

It was previously shown by Sasaki[26,27] and by our research group[28,29] that oxetane monomers exhibit long induction periods during photoinitiated cationic polymerization. Sasaki suggested that the extended induction period is the consequence of a slow ring-opening reaction of the initially formed secondary oxonium ion species [eq. (3), Scheme 1; i.e., $k_2 < k_3$]. Shown in Figure 10 is an example of this phenomenon in the photopolymerization of POX in the presence of an iodonium salt photoinitiator. Under the conditions of this experiment, an induction period of 7 min was observed. After that time, the spontaneous, rapid, exothermic polymerization of the oxetane takes place.
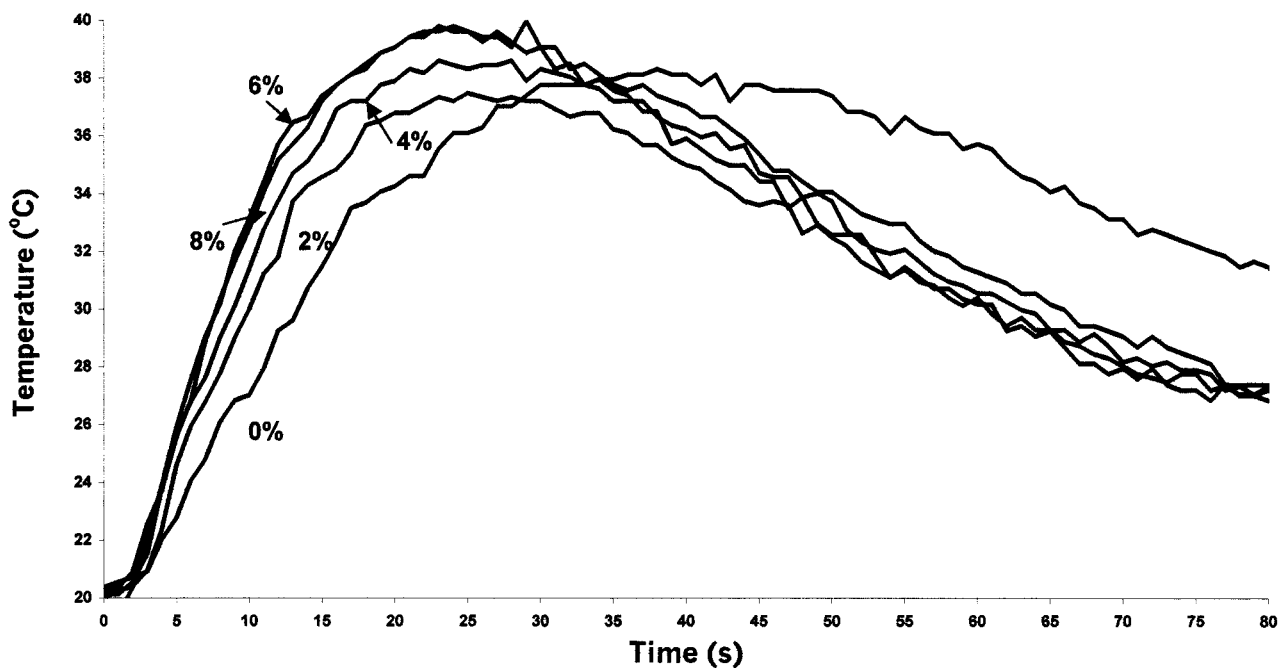
Figure 9 Effect of addition of limonene dioxide to 3,4-epoxycyclohexylmethyl 3′,4′-epoxycyclohexanecarboxylate (1.0 mol % IOC15 photoinitiator, 766 mJ cm^{-2} min^{-1}).

Because diaryliodonium salt photoinitiators have quantum yields of 0.4–0.8,[30,31] complete photolysis of the photoinitiator was achieved within the first several minutes of UV irradiation. Because protonation of the monomer by the superacid (HSbF$_6$) generated by pho-

tolysis of the photoinitiator is very rapid, the results are consistent with the formation of a metastable secondary oxonium species that undergoes slow ring opening by attack of the monomer. Once polymerization begins, considerable heat is generated (19–20 kcal
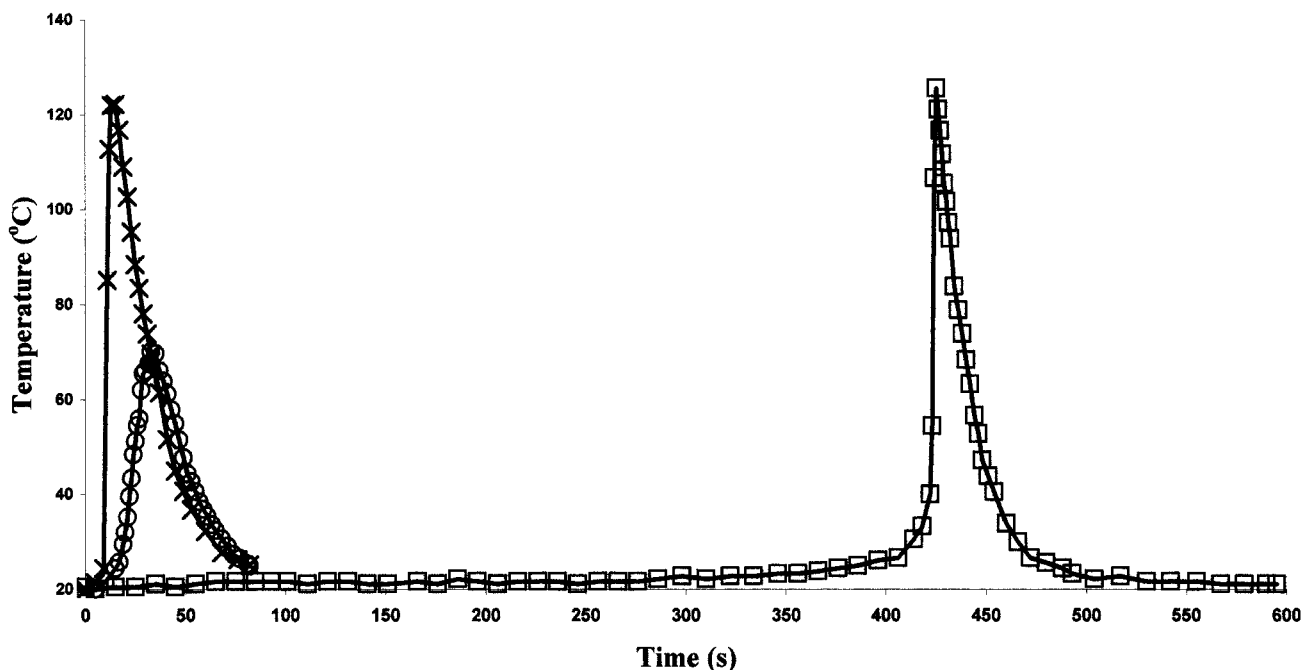
Figure 10 Acceleration of polymerization of POX by CHO: 0% (□); 2% (○); 10% (×) (1.0 mol % IOC15 photoinitiator, 498 mJ cm^{-2} min^{-1}).
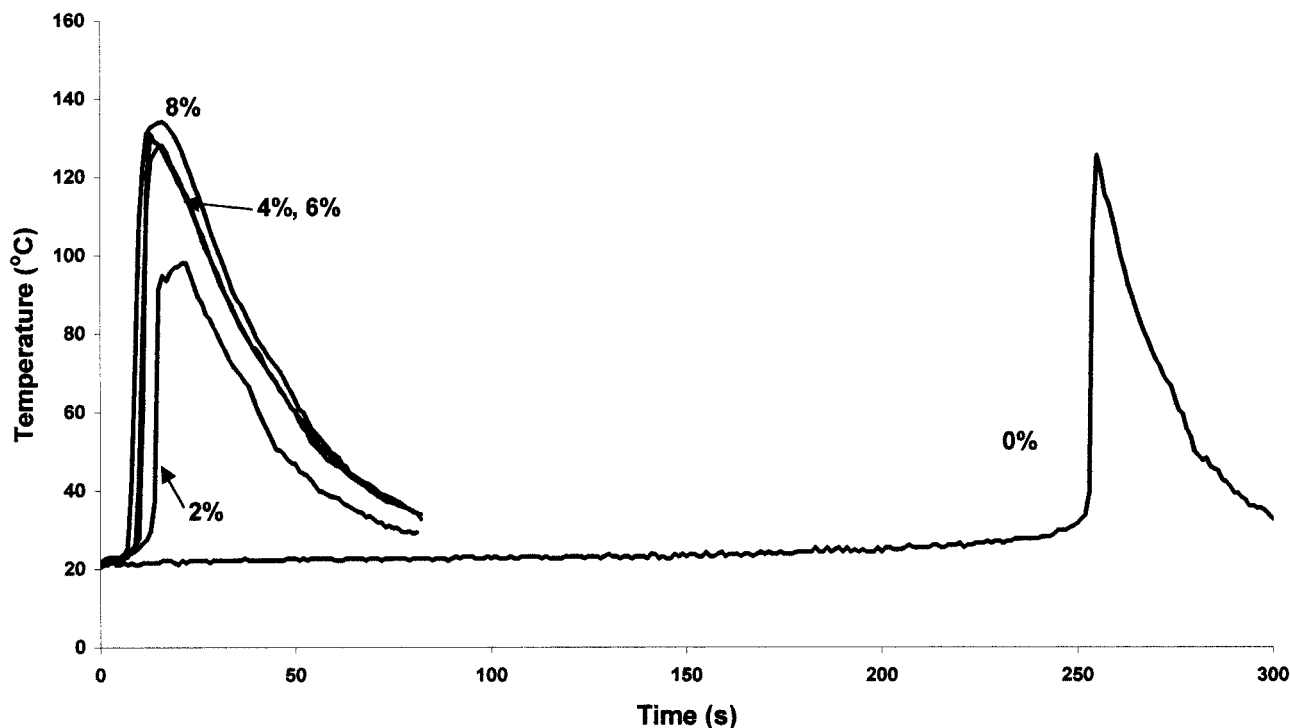
Figure 11   Acceleration of polymerization of POX by ERL-4221E (1.0 mol % IOC15 photoinitiator, 550 mJ cm^{-2} min^{-1}).

mol^{-1}),[32] leading to an autoaccelerated polymerization process. Due to their extended induction periods, oxetane monomers are generally ill suited to high-speed photopolymerizations used, for example, in photocurable printing inks. However, this problem could be resolved if the induction period can be effectively reduced or eliminated. As shown in Figure 10, the addition of small amounts of the epoxide monomer CHO rapidly accelerates the apparent polymerization rate of POX by markedly reducing the induction period. It was also of interest using OP to determine whether it might be possible to accelerate the rate of polymerization of POX with a less-reactive epoxide monomer. Compared to CHO, the photopolymerization of ERL-4221E is sluggish, as previously noted. However, as shown in Figure 11, the photopolymerization of POX is considerably accelerated in the presence of as little as 2 mol % (4 mol % epoxy groups) of ERL-4221E. Increasing the amount of ERL-4221E in the mixture produces a corresponding incremental decrease in the induction period.

Based on the above concept, it should also be possible to overcome the induction period of POX through the addition of a highly reactive vinyl ether monomer that forms a carbocation that can directly alkylate the cyclic ether to form a tertiary oxonium ion species. Shown in Figure 12 is an OP study of the photopolymerization of POX carried out in the presence of various amounts of triethylene glycol divinyl ether (DVE-3). As Figure 12 shows, the induction time

for the photopolymerization of POX is progressively reduced in the presence of increasing amounts of the divinyl ether.

XDO is a difunctional oxetane monomer that incorporates benzylic ether groups. This monomer also exhibits very poor photoresponse to UV light in the presence of onium salt photoinitiators. Figure 13 shows the effect on the photopolymerization of XDO upon the addition of different amounts of CHO to this monomer. No polymerization of XDO is observed, even after more than 12 min UV irradiation, at a light intensity of 930 mJ cm^{-2} min^{-1}. The addition of 6 and 10 mol % of CHO dramatically accelerates the polymerization of XDO, whereas 2.0 mol % CHO produces a barely observable effect on the polymerization rate.

Effect of humidity on the cationic photopolymerization of various monomers

Cationic polymerizations in general, and the corresponding photoinitiated polymerizations in particular, are sensitive to various environmental contaminants including bases, water, and alcohols. The most ubiquitous of these is water. Although cationic photopolymerizations are cited as being advantageous in many applications because they can be carried out in air, often it is not appreciated that different levels of water present as humidity can have an appreciable effect on the course of these reactions. There has been considerable discussion in the literature concerning
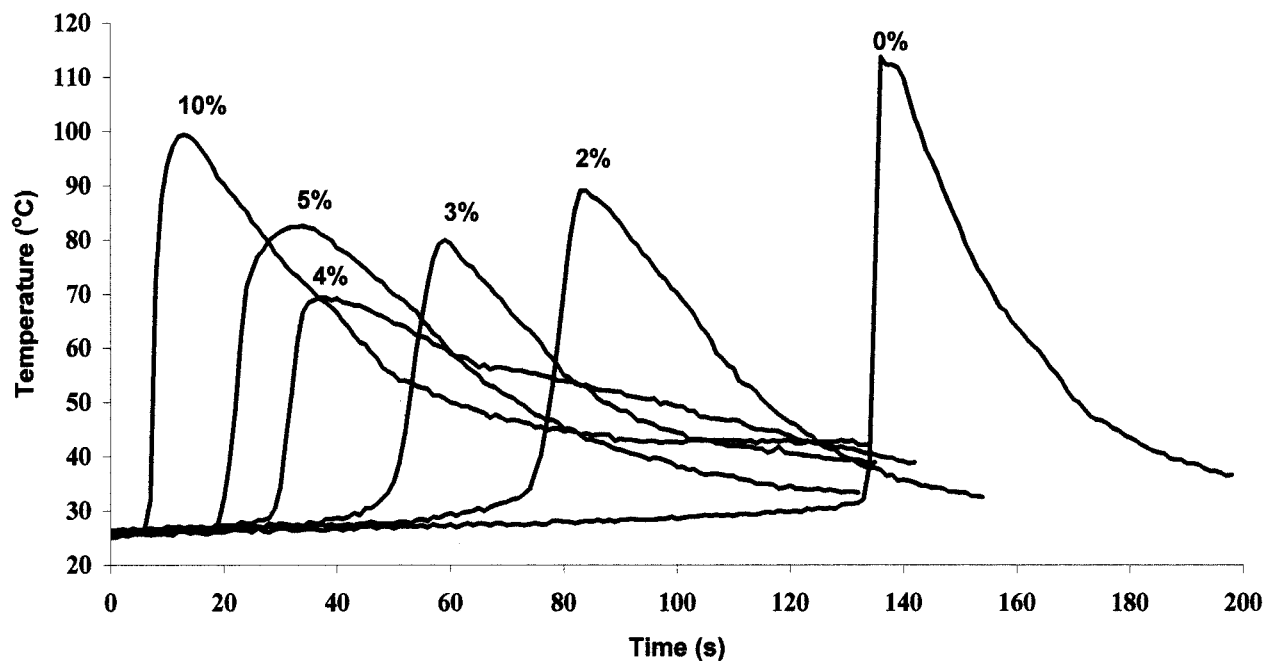
Figure 12 Effect of addition of DVE-3 on the photopolymerization of POX (1.0 mol % IOC10 photoinitiator, 342 mJ cm^{-2} min^{-1}).

the effect of humidity on the photoinduced ring-opening polymerizations of epoxides and on the polymerization of vinyl ether monomers.[35] The development of the OP technique offers the opportunity for conveniently obtaining useful data on the effects of water on these photopolymerization systems. Experiments were carried out at various levels of relative humidity in the closed cabinet of the OP instrument by passing air through a water bubbler until the desired relative humidity level was obtained.

Figure 14 shows the effect of two levels of relative humidity on the photoinitiated cationic polymeriza-
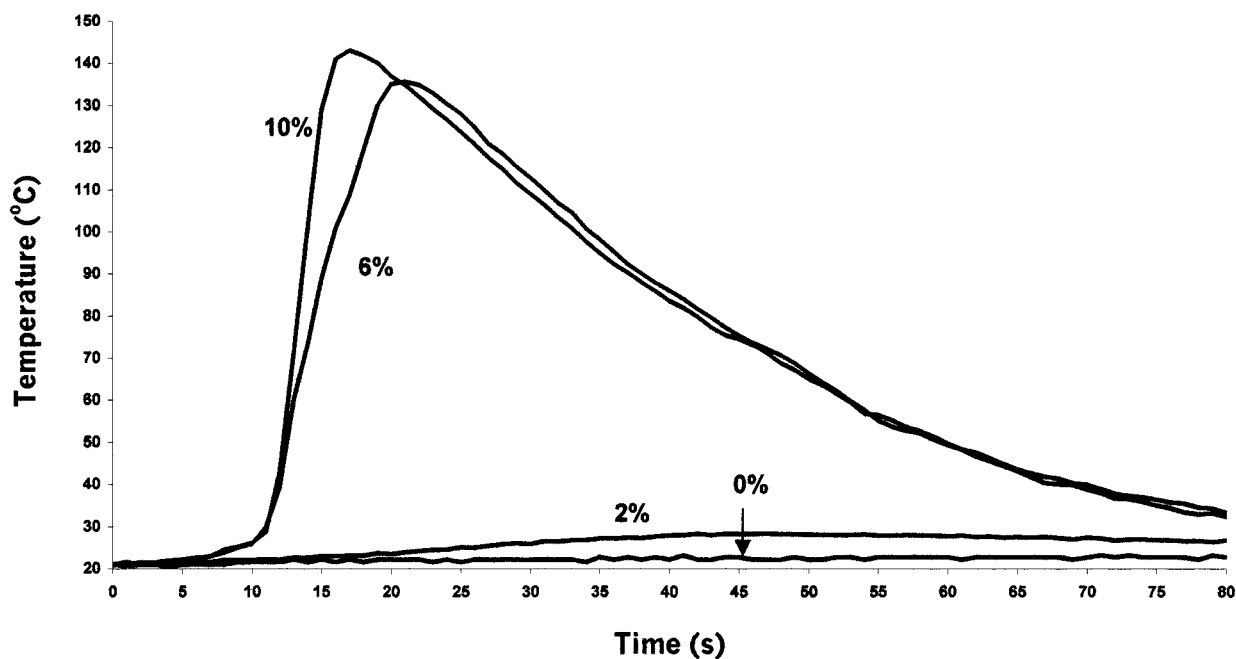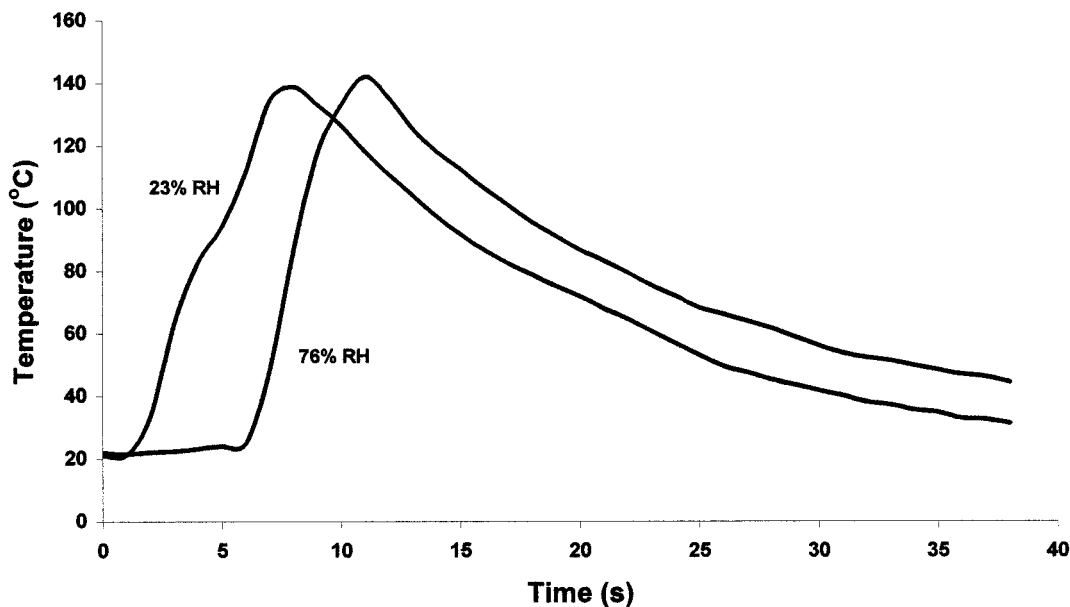

Figure 13 Acceleration of photopolymerization of XDO in the presence of CHO (1.0 mol % IOC15 photoinitiator, 930 mJ cm^{-2} min^{-1}).

Figure 14 OP study of the effect of relative humidities of 23 and 76% on the photopolymerization of CHO (1.0 mol % IOC15 photoinitiator, 285 mJ cm^{-2} min^{-1}).

tion of cyclohexene oxide. One can see an induction period in the polymerizations at both humidity levels. However, at the higher level (76%) there is a significant extension of the induction period to approximately 7 s. Overall, water is an inhibitor in the photopolymerization of CHO. Quite different and more complex behavior is noted in the case of the photopo-

lymerization of ERL-4221E, shown in Figure 15. When this polymerization was carried out at 24% relative humidity, a rather slow polymerization was noted after a very short induction period, along with only a very modest temperature increase from ambient to 43°C. When the same photopolymerization was carried out at 80% relative humidity, the induction period
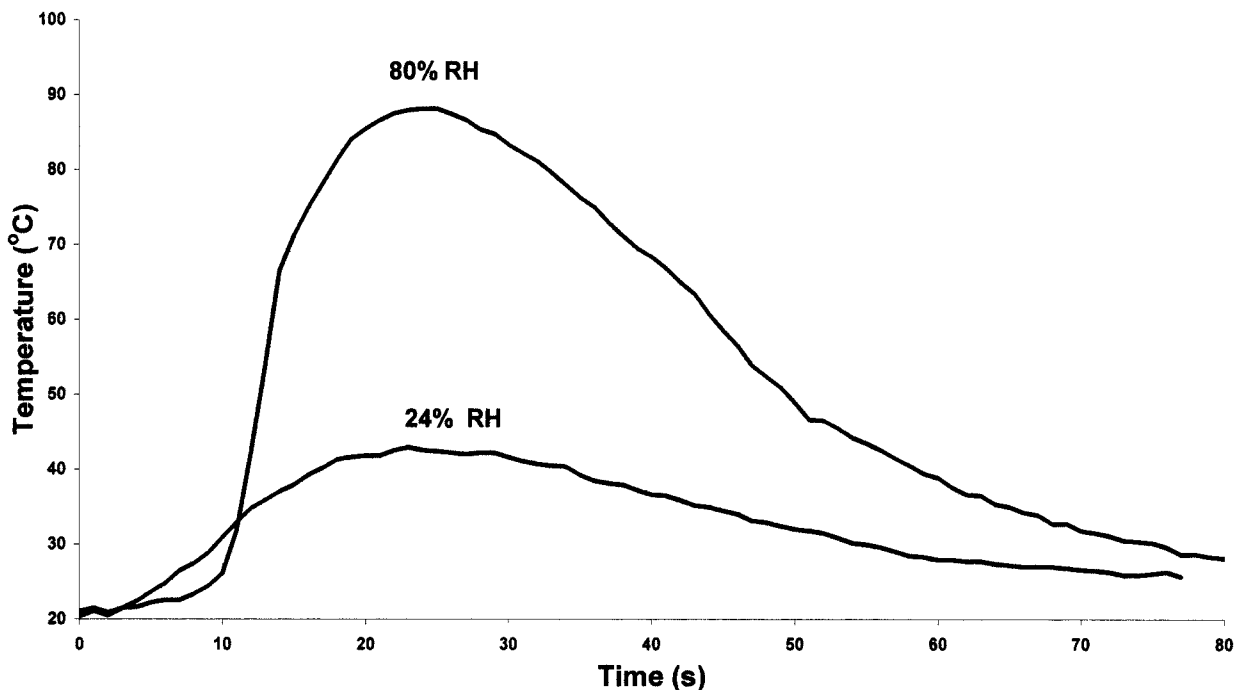
Figure 15 Effects of humidity on the photoinitiated polymerization of ERL-4221E (1.0 mol % IOC15 photoinitiator, 1039 mJ cm^{-2} min^{-1}).
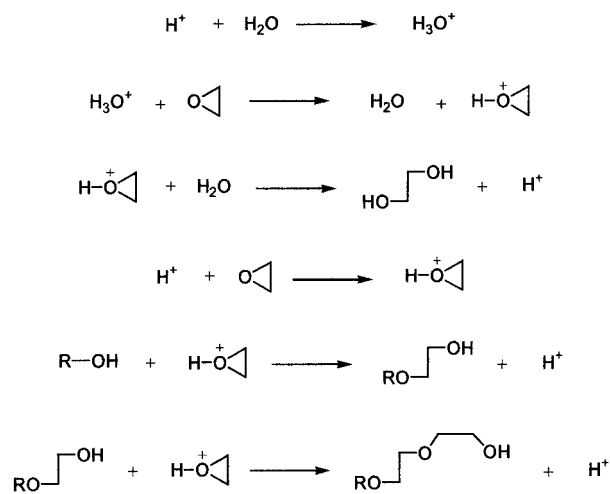
Scheme 2

was dramatically lengthened, but once the polymerization took place it occurred rapidly, with the sample temperature reaching 88°C. Several phenomena appear to be taking place with somewhat offsetting effects. This is depicted in Scheme 2 (anions are omitted for simplicity).

First, water behaves as an inhibitor. When it is present, the Brønsted acid generated through photolysis of the onium salt photoinitiator reacts with it preferentially to generate the hydronium ion [eq. (5)]. Subsequently, water reacts with the epoxide in an acid-catalyzed addition reaction to generate a diol and liberate a proton, as shown in eqs. (6) and (7). In the course of this latter reaction, water is removed from the reaction

mixture and alcohol groups are formed. Once this has occurred and irradiation continues with the liberation of more photogenerated acid, protonation of the epoxide monomer begins to take place [eq. (8)]. Finally, the nucleophilic alcohol groups react with the protonated monomer to form ether linkages and to generate more alcohol groups [eq. (9)[rsqb]. This reaction repeats [eq. (10)] as chain growth continues by a classical "activated monomer" polymerization, as described by Penczek et al.[34–38] The activated monomer reaction is more rapid than the usual repetitive addition of an epoxide monomer to the growing oxonium ion chain end reaction [Scheme 1, eq. (4)], given that proton transfer is a very rapid process and also because addition of alcohols to the reactive chain end has fewer steric constraints than the corresponding addition of an epoxide ring.

An additional effect is also operative in the polymerization of the difunctional monomer ERL-4221E, which gives a crosslinked network on photopolymerization. During polymerization, the liquid monomer is transformed into a solid. Crosslinking and solidification quickly immobilizes the growing chain ends that are bound to the network, thus impeding their further reaction with monomer because of restricted diffusion. This appears to be another reason for the sluggish behavior of ERL-4221E. The addition of water results in facile chain transfer, as shown in Scheme 2. This results in a delay of the onset of gelation, permitting the reaction to proceed to higher conversion.

A similar effect was observed and is depicted in Figure 16 for the photopolymerization of PC-1000 [bis-
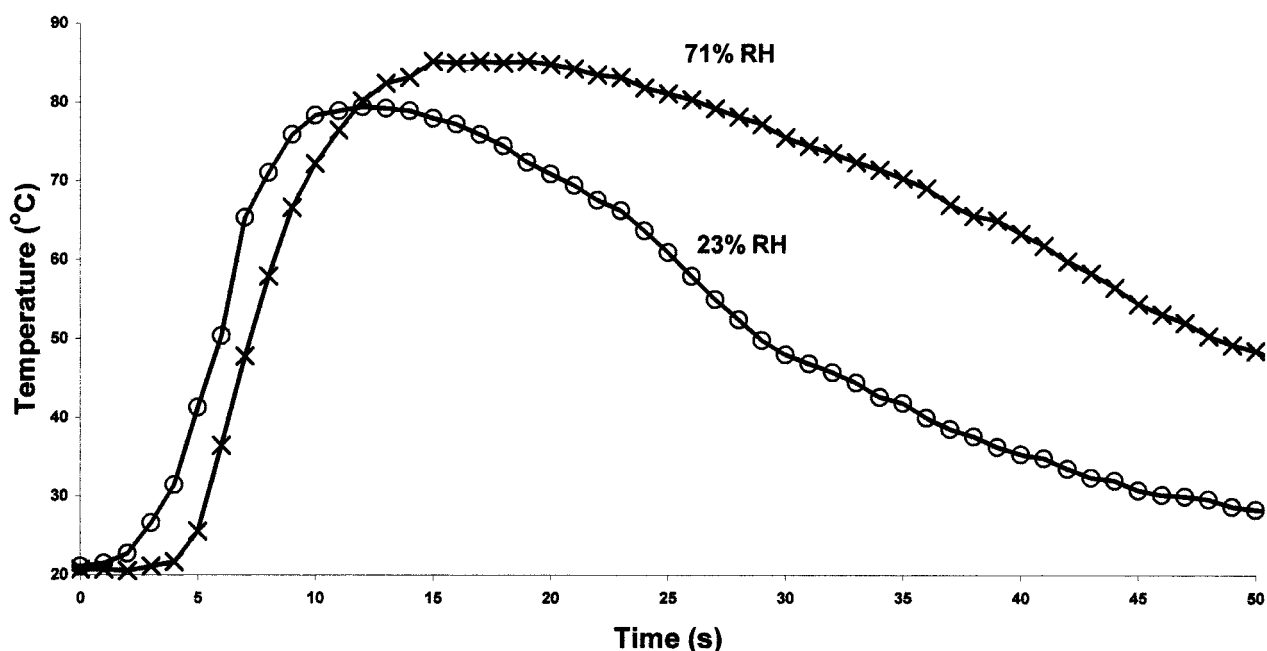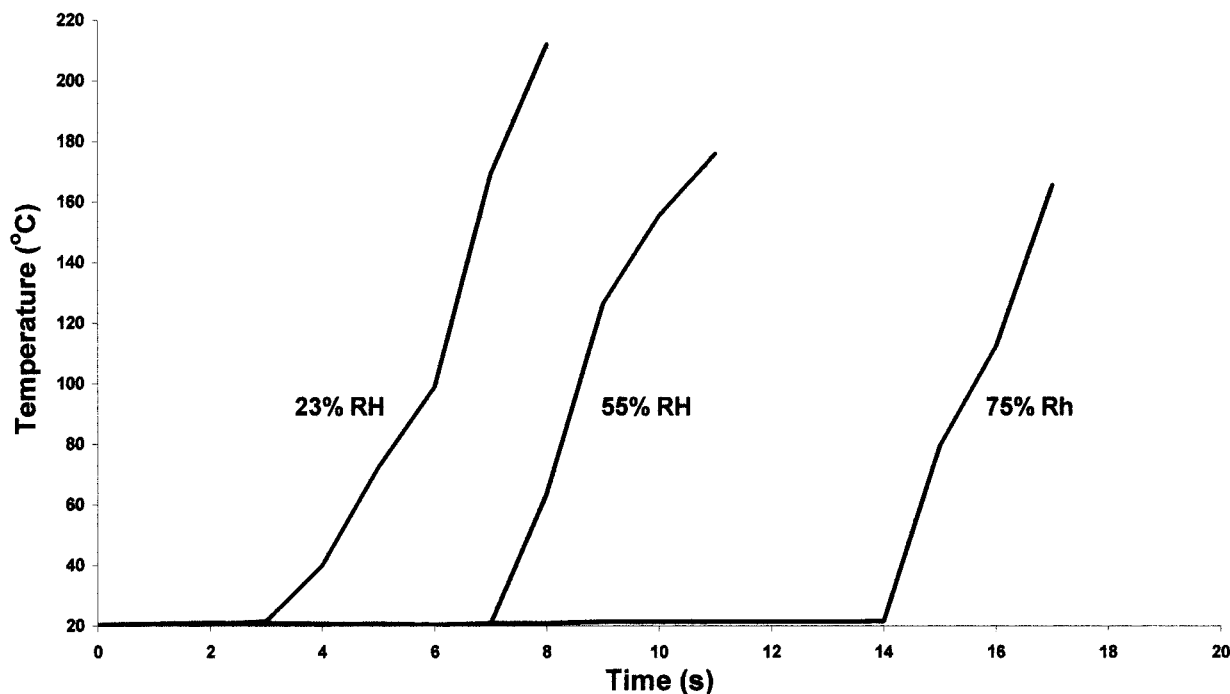

Figure 16 Effect of humidity on the photopolymerization of PC-1000 (1.0 mol % IOC15 photoinitiator, 331 mJ cm^{-2} min^{-1}).

Figure 17 Photopolymerization of 1,6-hexanediol divinyl ether in the presence of relative humidities of 23, 55, and 75% (1.0 mol % IOC15 photoinitiator, 345 mJ cm^{-2} min^{-1}).

1,2(2-(3,4-epoxycyclohexylethyl))-1,1,2,2-tetramethyl-disiloxane]. At high (71%) relative humidity the photopolymerization of this monomer exhibits an increased inhibition period, but with a higher peak temperature and more sustained polymerization than when the polymerization is carried out at lower (23%) relative humidity. The effects of humidity on the photopolymerization of PC-1000 appear to be less than those observed with ERL-4221E, possibly because the former monomer is considerably less hydrophilic than the latter and undergoes both slower and lower moisture uptake on equilibration with the environment.

Vinyl ethers undergo facile highly exothermic photopolymerization in the presence of onium salt photoinitiators. However, these monomers are exceptionally sensitive to the presence of traces of water, given that the active species involved in polymerization is a carbocation. Figure 17 depicts the effect of various levels of relative humidity on the cationic photopolymerization of 1,6-hexanediol divinyl ether. The curves in this figure are truncated because the polymerizations are extremely vigorous and the sample undergoes considerable decomposition during polymerization. There is a progressive increase in the induction period as the relative humidity is increased. At the same time the reactivity of the system is not appreciably affected. Vinyl ethers undergo acid-catalyzed addition of water to form hemiacetals, as depicted in eq. (11) of Scheme 3.[39] The hemiacetals that are formed react further to give an aldehyde and an alcohol [eq. (12)]. These reactions consume water during the early phases of the reaction. Once water is depleted in the system, polymerization of the remaining monomer proceeds vigorously.

CONCLUSIONS

Optical pyrometry is a convenient analytical method for investigating photoinitiated cationic polymerizations. By use of this method, the effects of photoinitiator structure on the photopolymerizations of various cyclic ether monomers were investigated. A study of the influence of monomer structure on the polymerization of various epoxide and oxetane monomers was also conducted. It was observed that the photopolymerizations of those monomers that display slow rates of polymerization, attributed to long induction periods, can be accelerated by the addition of a small amount of a more reactive monomer. In such poly-
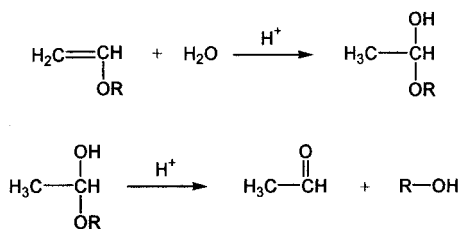
Scheme 3

merizations, the slowest step of the polymerization reaction involves the ring opening of the secondary oxonium ion by the cyclic ether monomer. Increasing the rate of this reaction by the addition of a more reactive monomer increases the overall polymerization rate of the monomer. The presence of water during a photoinduced cationic ring-opening polymerization can have several effects. Generally, the presence of water is inhibiting for the polymerization of these monomers. However, in a crosslinking polymerization, an increase in the rate of polymerization may be realized because of mobilization of the reactive cationic species arising from chain transfer and suppression of the gel point. The results obtained in this study provide support for the value of optical pyrometry as a useful tool for monitoring rapid photopolymerization reactions.

References

1. Decker, C.; Moussa, K. Eur Polym Mater 1990, 26, 393.
2. Decker, C.; Moussa, K. Makromol Chem 1990, 191, 963.
3. Decker, C. J Polym Sci Part A: Polym Chem 1992, 30, 913.
4. Moore, J. E. In: UV Curing: Science and Technology; Pappas, S. P., Ed.; Technology Marketing Corp.: Stamford, CT, 1978; p. 134.
5. Hoyle, C. E. In: Radiation Curing Science and Technology; Papas, S. P., Ed.; Plenum Press: New York, 1992; p. 57.
6. Falk, B.; Vallinas, S. M.; Crivello, J. V. J Polym Sci Part A: Polym Chem 2003, 41, 579.
7. Crivello, J. V.; Lee, J. L. J Polym Sci Polym Chem Ed 1989, 27, 3951.
8. Crivello, J. V.; Ahn, J. J Poly Sci Polym Chem Ed. 2003, 41, 2570.
9. Crivello, J. V.; Lam, J. H. W. J Polym Sci Polym Chem Ed. 1980, 18, 2697.
10. Crivello, J. V.; Jiang, F.; Ma, J. Polym Prepr 2003, 44, 13.
11. Crivello, J. V.; Kong, S. Macromolecules 2000, 33, 825.
12. Crivello, J. V.; Kong, S. Macromolecules 2000, 33, 833.
13. Crivello, J. V.; Lee, J. L. Macromolecules 1983, 16, 864.
14. Crivello, J. V.; Ahn, J. J Poly Sci Polym Chem Ed 2003, 41, 2570.
15. Crivello, J. V.; Ahn, J. J Poly Sci Polym Chem Ed 2003, 41, 2556.
16. Koleske, J. V. In: Proceedings of RadTech '88 North America Conference, New Orleans, LA, April 24–28, 1988; p. 353.
17. Crivello, J. V.; Linzer, V. Polimery (Warsaw) 1998, 68, 661; Chem Abstr 1999, 130, 182793u.
18. Plotkin, J. S.; Dougherty, J. A.; Miller, M.; Narayanan, K. S.; Vara, F. J. In: Proceedings of RadTech '92 North America Conference, Boston, MA, April 26–30, 1992; Vol. 1, p. 553.
19. Crivello, J. V.; Lee, J. L. Polym Mater Sci Eng Prepr 1989, 60, 217.
20. Crivello, J. V.; Lee, J. L. Radiation Curing of Polymeric Materials; Hoyle, C. E.; Kinstle, J. F., Eds.; ACS Symposium Series 417; American Chemical Society: Washington, DC, 1989; p. 398.
21. Crivello, J. V.; Lee, J. L. In: Proceedings of the RadTech '90 North America Conference, Chicago, IL, March 25, 1990; p. 432.
22. Crivello, J. V.; Lam, J. H. W.; Moore, J. E.; Schroeter, S. H. J Radiat Curing 1978, 5, 2.
23. Sinka, J. V.; Mazzoni, D. In: Proceedings of RadTech '88 North America Conference, New Orleans, LA, April 24–28, 1988; p. 378.
24. Crivello, J. V.; Varlemann, U. J Polym Sci Polym Chem Ed 1995, 33, 2463.
25. Crivello, J. V.; Varlemann, U. J Polym Sci Polym Chem Ed 1995, 33, 2473.
26. Sasaki, H. In: Proceedings of RadTech 2000 Technical Conference, Baltimore, MD, April 9–12, 2000; p. 61.
27. Kato, H.; Sasaki, H. Photoinitiated Polymerization; ACS Symposium Series 847; American Chemical Society: Washington, DC, 2003; p. 285.
28. Crivello, J. V.; Falk, B.; Zonca, M. R., Jr. J Polym Sci Polym Chem Ed, to appear.
29. Crivello, J. V.; Sasaki, H. J Macromol Sci Pure Appl Chem 1993, A30, 189.
30. Crivello, J. V. In: Ring Opening Polymerization; Brunelle, D. J., Ed.; Hanser: Munich, 1993; p. 157.
31. Selvaraju, C.; Sivakumar, A.; Ramamurthy, P. J Photochem Photobiol A Chem 2001, 138, 213.
32. Bandrup, J.; Immergut, E. H. Polymer Handbook; Interscience: New York, 1966; pp. II–374.
33. Eaton, R. F.; Hanrahan, B. D.; Braddock, J. K. In: Proceedings of RadTech '90 North America Conference, Chicago, IL, March 25–29, 1990; Vol. 1, p. 353.
34. Penczek, S.; Kubisa, P.; Matyjaszewski, K.; Szmanski, R. Pure Appl Chem 1984, 140.
35. Brzezinska, K.; Szymanski, R.; Kubisa, P.; Penczek, S. Makromol Chem Rapid Commun 1986, 7, 1.
36. Penczek, S.; Kubisa, P.; Szymanski, R. Makromol Chem Macromol Symp 1986, 3, 203.
37. Wojtania, M.; Kubisa, P.; Penczek, S. Makromol Chem Macromol Symp 1986, 6, 201.
38. Kubisa, P. Makromol Chem Macromol Symp 1988, 13/14, 203.
39. Schildknecht, C. E. Vinyl and Related Polymers; Wiley: New York, 1952; p. 596.